Since January 2020 Elsevier has created a COVID-19 resource centre with free information in English and Mandarin on the novel coronavirus COVID-19. The COVID-19 resource centre is hosted on Elsevier Connect, the company's public news and information website.

Process Biochemistry 121 (2022) 656–660

Contents lists available at ScienceDirect

Process Biochemistry

journal homepage: www.elsevier.com/locate/procbio

Charge transport properties of SARS-CoV-2 Delta variant (B.1.617.2)

Lijun He *, Zhiyang Xie, Xing Long, Chaopeng Zhang, Chengyun He, Boyang Zhao, Fei Qi, Nan Zhang

The School of Optoelectronic Engineering, Chongqing University of Posts and Telecommunications, Chongqing 400065, China

ARTICLE INFO

Keywords:
Conductance
SARS-CoV-2
B.1.617.2 (delta)
RNA:DNA hybrids

ABSTRACT

The B.1.617.2 (Delta) variant of concern is causing a new wave of infections in many countries. In order to better understand the changes of the SARS-CoV-2 mutation at the genetic level, we selected six mutations in the S region of the Delta variant compared with the native SARS-CoV-2 and get the conductance information of these six short RNA oligonucleotides groups by construct RNA: DNA hybrids. The electronic characteristics are investigated by the combination of density functional theory and non-equilibrium Green's function formulation with decoherence. We found that conductance is very sensitive to small changes in virus sequence. Among the 6 mutations in the Delta S region, D950N shows the largest change in relative conductance, reaching a surprising 4104.75%. These results provide new insights into the Delta variant from the perspective of its electrical properties. This may be a new method to distinguish virus variation and possess great research prospects.

1. Introduction

SARS-CoV-2 is the virus that causes COVID-19 and B.1.617.2 is one of the variants of SARS-CoV-2 which was first detected in India [1]. B.1.617.2 is also named Delta by WHO (World Health Organization) for easy discussions in the public. The Delta variant acquires multiple mutations which can affect viral properties such as infectivity and immune resistance. For example, it has been reported that L452R (mutation in the 452th amino acid on spike protein from Leucine (L) to Arginine (R)) helps the virus escaping from HLA-A24-mediated cellular immunity and increasing binding affinity to ACE2 [2]. A recent article also pointed out that P681R can make the virus enter cells more effectively [3]. Because of its increase in transmissibility and more severe disease, the Delta variant rapidly spread during the second wave of COVID-19 in India, and it has spread to 78 countries [4].

The continuation of the spread of the highly transmissible SARS-CoV-2 Delta variant points out the significance of virus mutation research. Although a large number of researchers have studied the nature and infectivity of the Delta variant. But so far, few articles have studied the Delta variant from the perspective of it's electronic characteristics. SARS-CoV-2 is a positive-sense single-stranded RNA virus of about 30,000 base length. In recent years, some studies have studied the charge transport in nanomaterials [5,6] and the electrical properties of cytosine hydroxymethylated (Chm) DNA sequences [7]. A recent article found that single-molecule conductance techniques can be used to extract biologically relevant information from short RNA oligonucleotides by construct RNA:DNA hybrids [8]. So this paper has considered whether virus variation can be analyzed from the perspective of electrical characteristics. In this work, the charge transport properties of the Delta variant sequence with the native SARS-CoV-2 sequence are compared. We demonstrate that the conductance of RNA:DNA hybrids is highly sensitive to single nucleotide differences of Delta variant and native SARS-CoV-2.

2. Materials and methods

2.1. Obtain the sequence information of mutation site before calculation

The SARS-CoV-2 mutates all the time, It has been found that more than 10 mutations have occurred on Delta variant compared with the original SARS-CoV-2 (MN908947.3, one of the initial isolates of SARS-CoV-2 and serves as a reference sequence). But this work focuses on the mutations in its spike (S) protein because the SARS-CoV-2 spike (S) glycoprotein is exposed at the surface of the virus and mediates entry into host cells. S is the main target of neutralizing antibodies and the focus of most vaccines [9,10]. We get the mutation information from the 2019 Novel Coronavirus Resource and collected six of the most critical mutations in the S region [11–13]. The key information of the six

* Corresponding author.
E-mail addresses: helijun4@126.com, helj@cqupt.edu.cn (L. He).

https://doi.org/10.1016/j.procbio.2022.08.010
Received 11 February 2022; Received in revised form 21 July 2022; Accepted 8 August 2022
Available online 10 August 2022

Table 1
The key information of the six mutations of Delta variant (compared with MN908947.3).

Genome position	Base change	Gene	Amino acids change	Before mutation	After Mutation
21,618	C -> G	S	T19R	UUACAAC	UUAGAAC
22,917	U -> G	S	L452R	ACCUGUA	ACCGGUA
22,995	C -> A	S	T478K	GCACACC	GCAAACC
23,403	A -> G	S	D614G	AGGAUGU	AGGGUGU
23,604	C -> G	S	P681R	CUCCUCG	CUCGUCG
24,410	G -> A	S	D950N	CAAGAUG	CAAAAUG

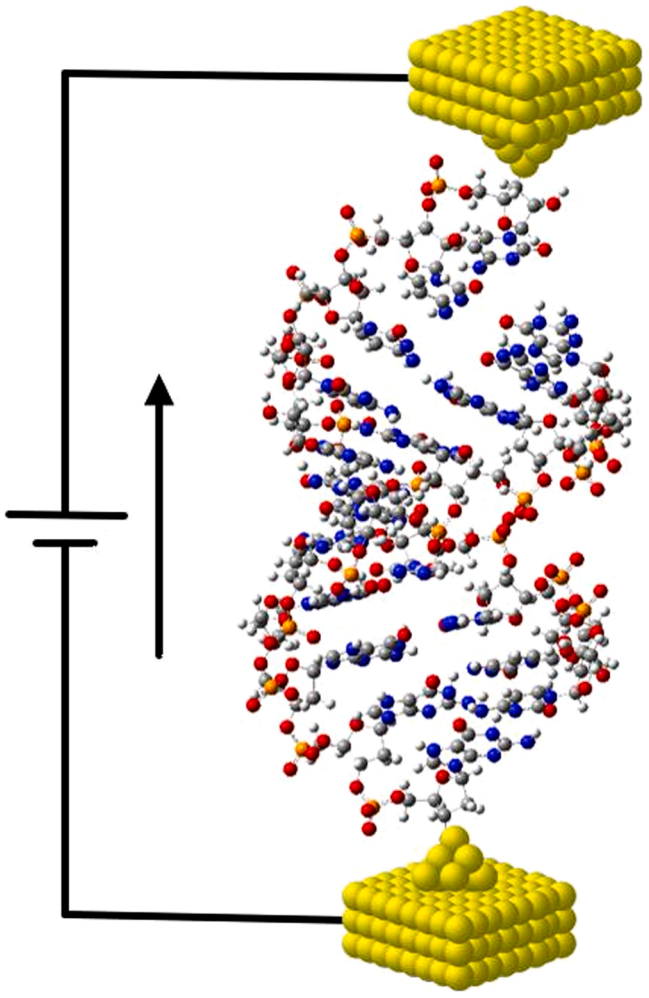

Fig. 1. Idealized schematic of electrical property experimental setup. The RNA: DNA hybrids molecule is bounded between two yellow gold electrodes.

mutations of the Delta variant are shown in Table 1. We took three bases from the base mutation site to the left and right to study the difference of SARS-CoV-2 electrical properties before and after mutation. Double-stranded RNA: DNA hybrids sequences with a total length of seven base pairs are selected, respectively. The Idealized schematic of RNA:DNA hybrids based electrical measurement system is shown in Fig. 1. The RNA:DNA hybrids molecule is bounded between two yellow gold electrodes and electrons are injected and extracted into the DNA sequence through the 3′ end.

2.2. Construct the RNA: DNA hybrid structure

The Nucleic Acid Builder (NAB) software package can be used to construct various nucleic acid structures. Research has found that the RNA: DNA hybrid molecules are all in an A-form-like configuration, so we first constructed A-form-RNA and A-form-DNA according to the above virus sequence, and then combined them into RNA: DNA hybrid structure by NAB. It is worth noting that in this work, we study the charge transport of pure static nucleic acids without considering the influence of counter ions.

2.3. DFT and non-equilibrium Green's function

After obtaining the RNA: DNA hybrid molecular structure of virus sequences, the density functional theory (DFT) and non-equilibrium Green's function approach including decoherence [14–17] are employed to calculate the electrical information of different molecular structures. First of all, the DFT calculations were performed by Gaussian09 [18] and we chose B3LYP functional and 6–31 G (d, p) basis set. In order to be closer to the real experimental environment, the polarization continuum model (PCM) is used to consider the influence of solvent (water). After DFT calculations we will obtained the Hamiltonian and the overlap matrices of the calculated molecular structure and then use Löwdin transformation [19] method to convert it into orthogonalized Hamiltonian matrix.

So far, we have obtained the orthogonalized Hamiltonian matrix of the system by using DFT, next, the Hamiltonian matrix is calculated to obtain the electrical information such as conductance, transmission probability of virus sequence by the non-equilibrium Green's function formulation with decoherence. the retarded Green functional can be calculated by:

$$G_M^r(E) = \frac{1}{EI_{MM} - H_{MM} - \sum_L^r - \sum_R^r - \sum_B} \tag{1}$$

Where E is the energy, I_{MM} is identity matrix of M*M, H is the Hamiltonian of the molecule, $\sum_L^r$ and $\sum_R^r$ are the self energy matrices from the left (right) contact. In order to incorporate decoherence into the transmission model. $\sum_B$is used to represents the self energy matrices generated by the Buttiker probes.

The transmission probability can be obtained by:

$$T_{eff} = \Gamma_L G^r \Gamma_R G^a + \sum_{i,j=1}^{N_b} \Gamma_L G^r \Gamma_i G^a W_{ij}^{-1} \Gamma_L G^r \Gamma_j G^a \tag{2}$$

Where $\Gamma_L(R)$ is the coupling between the Intermediate molecule and the left or right contacts. Here, contact coupling between the molecule and the two electrodes is set to 100 meV. G^r is the retarded Green functional in Eq. (1). G^a is the advanced Green functional. N_b represents the number of Büttiker probes. The W_{ij}-1 is the inverse of W_{ij}. W_{ij}= [(1-R_{ii})δ_{ij}-$\Gamma_i G r \Gamma_j G_a$(1-$\delta_{ij}$)], where R_{ii} is the reflection probability at probe i. In this article, the decoherence rate is set to 10 meV.

After obtaining the transmission probability, the conductance of the molecule can be get by:

$$G(E_f) = G_0 \int dE T_{eff}(E) \frac{-\partial f(E - E_f)}{\partial E} \tag{3}$$

Where E_f is the Fermi functional. G_0 is The quantum conductance and $G_0 = 2e^2/h \approx 7.75 \times 10^{-5}$S. T_{eff} is the transmission probability we have calculated above.

In our previous publication, we have define a parameter to better understand the relative change in conductance upon mutation [20]. Here, we also use$\delta G$to make It more intuitively to shows the change of conductivity before and after virus mutation. whereG_{UM}represents the conductance of the naive sars-cov-2 and$G_M$represents the conductance of the Delta variant.

$$\delta G = \frac{G_M - G_{UM}}{G_{UM}} \times 100 \tag{4}$$

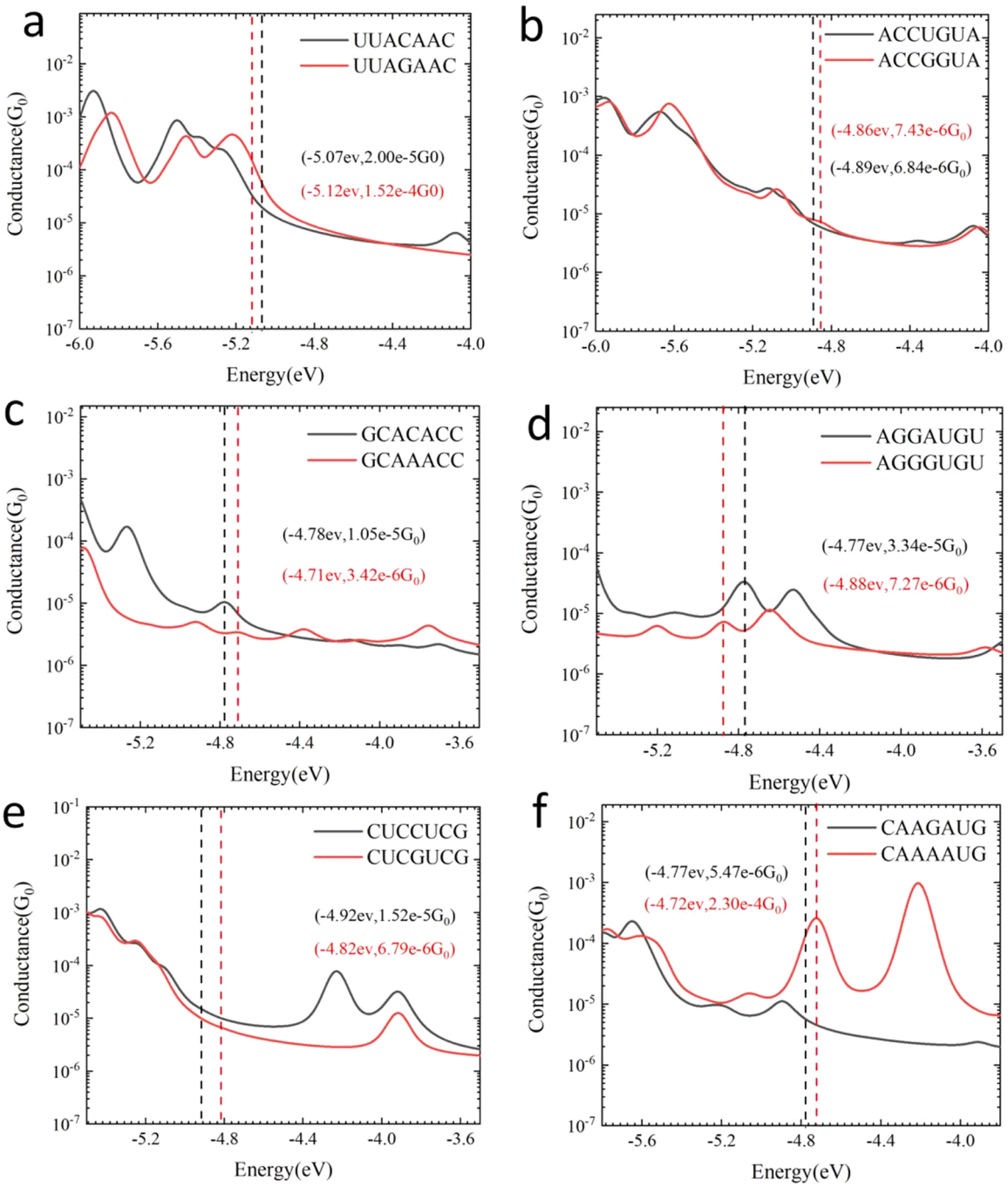

Fig. 2. The conductance in the vicinity of HOMO for virus sequences of the six mutations of Delta variant: (a) T19R, (b) L452R, (c) T478K, (d) D614G, (e) P681R, (f) D950N. Dash line is the position of HOMO energy level and black represents the non-mutated SARS-CoV-2, red represents the Delta variant.

3. Results and discussion

For the convenience of discussion, we will use amino acid changes to refer to specific virus sequences in the following analysis, such as pre-D614G (pre-mutation) represent the sequence of AGGAUGU and D614G represent the sequence of AGGGUGU (refer to Table 1). Fig. 2 shows the conductance variation with energy in the vicinity of respective HOMO (Highest Occupied Molecular Orbital) energy for the six mutation sites of the Delta variant. It is easy to see that compared with the native SARS-CoV-2 sequence , the conductance of the Delta variant has changed significantly in all six mutation cases. The conductance variation of pre-T19R and T19R is shown in Fig. 2a. In this mutation, a C base is changed to G base. After mutation, the conductance increased from 2.00×10^{-5} G_0 to 1.52×10^{-4} G_0, that is, δG= 660%. Fig. 2b shows the conductance of pre-L452R and L452R. Same as T19R, after mutation, the conductance of L452R increased from 6.84×10^{-6} G_0 to 7.43×10^{-6} G_0. theδGhere is only 8.63%, which is the minimum conductance change among all the six mutations studied. Fig. 2c presents the conductance variation of virus sequence when a C base is changed to A base. the conductance decreased from 1.05×10^{-5} G_0 to 3.42×10^{-6} G_0, that is,δG= −67.43%. We can see that there are three successive AT base pairs in the Delta sequence after mutation and there have been research findings that AT base pair acts as a barrier and GC base pair as a well for hole transport in DNA (dsDNA) duplexes [21]. So we believe that AT base pair has the same barrier properties in RNA:DNA hybrids as dsDNA. Fig. 2d shows the conductance variation of pre-D614G and D614G. The

Table 2
The transmission, conductance, under the six mutations of the Delta variant.

Virus Sequence	Sequence	HOMO (eV)	Cond (G_0)	Teff (HOMO)	ΔG
pre-T19R	UUACAAC	-5.07	2.00E-05	1.77E-05	660%
T19R	UUAGAAC	-5.12	1.52E-04	7.01E-05	
pre-L452R	ACCUGUA	-4.89	6.84E-06	6.77E-06	8.63%
L452R	ACCGGUA	-4.86	7.43E-06	9.29E-06	
pre-T478K	GCACACC	-4.78	1.05E-05	2.68E-05	-67.43%
T478K	GCAAACC	-4.71	3.42E-06	4.31E-06	
pre-D614G	AGGAUGU	-4.77	3.34E-05	7.47E-05	-78.23%
D614G	AGGGUGU	-4.88	7.27E-06	1.61E-05	
pre-P681R	CUCCUCG	-4.92	1.52E-05	1.47E-05	-55.33%
P681R	CUCGUCG	-4.82	6.79E-06	6.56E-06	
pre-D950N	CAAGAUG	-4.77	5.47E-06	4.90E-06	4104.75%
D950N	CAAAAUG	-4.72	2.30E-04	7.60E-04	

conductance at HOMO before the mutation is 3.34×10^{-5} G_0 and 7.27×10^{-6} G_0 after the mutation, that is,$\delta G = -78.23\%$. the reason why the conductance becomes smaller after mutation is the pre-D614G possess higher HOMO decreasing the activation energy for a charge to move between the electrodes and the bridge [8]. Fig. 2e shows the conductance of P681R decreased from 1.52×10^{-5} G_0 to 6.79×10^{-6} G_0 ($\delta G = -55.33\%$) compared with pre-P681R and Fig. 2f shows the conductance of D950N increased from 5.47×10^{-6} G_0 to 2.30×10^{-4} G_0 ($\delta G = 4104.75\%$) compared with pre-D950N. The transmission in the vicinity of respective HOMO energy for the six mutation sites of the Delta variant is also recorded in Table 2 and which shows the same trend as the conductance.

In Fig. 2f, we can obviously see that the conductance of the virus changes much more before and after mutation compared with the other five cases. theδGvalue reached a surprising 4104.75%. This shows that it is more possible to detect this mutation by measuring sequence conductivity. To provide additional verification that why D950N possesses higher conductance than pre-D950N. here we also performed ab initio electronic structure calculations of the 7 bp RNA:DNA duplex using the Gaussian 09 W software package and the Multiwfn [22] to examine the delocalization of the HOMO level along with the base stack. Fig. 3 plots the HOMO isosurface (isovalue $= 3 \times 10^{-3}$), Fig. 3a and Fig. 3b represent the HOMO isosurface of pre-D950N and D950N, respectively. and in Fig. 3 it is evident that a higher delocalization of the HOMO orbital in the D950N case. These results suggest that for a given number of bp's, the charge should transport more efficiently in the D950N case than in the pre-D950N case [23]. This fact is consistent with the conductance we calculate before.

4. Conclusion

In this work, we have investigated the electronic characteristics of Delta variant and native SARS-CoV-2 sequence by a combination of DFT and non-equilibrium Green's function including decoherence. These results provide new insights into the ongoing second wave of COVID-19. We demonstrate that the conductance is extremely responsive to small changes in the virus sequence, down to single-base modification. The underlying reason for this specificity originates may attribute to their conformational differences due to viral mutations. we have plots the HOMO isosurface which show that the HOMO level is more distributed along with the molecules in RNA:DNA duplexes of D950N, which suggests a higher conductance than pre-D950N. Given the obvious difference of conductance caused by mutation, this electrical measurement of SARS-CoV-2 may open the new door to single-molecule sensors with applications in fundamental biomedical research and COVID-19 diagnosis.

Data accessibility

The datasets used or analyzed during the current study are available from the corresponding author on reasonable request.

Declaration of Competing Interest

The authors declare that they have no conflict of interest.

Data availability

Data will be made available on request.

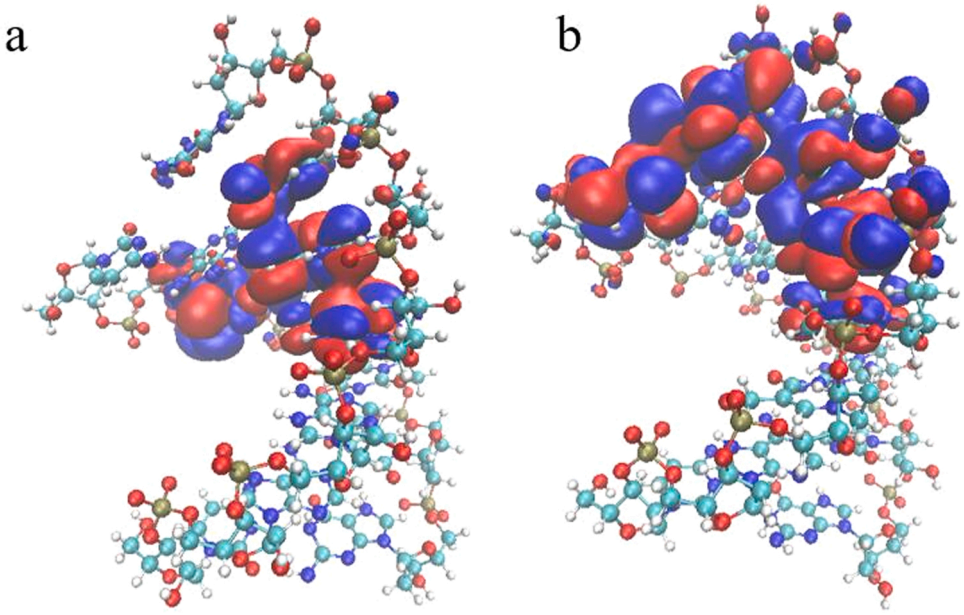

Fig. 3. 3D iso-surface plot of the HOMO orbital: (a) pre-D950N and (b) D950N, (blue and red colors represent positive and negative isosurfaces, respectively; isovalue $= 3 \times 10^{-3}$).

Acknowledgements

This work was supported by the China Scholarship Council Study Program for Young Backbone Teachers under grant no. 201707845017, the National Nature Science Foundation of China under grant no. 61804020, the Scientific and Technological Research Foundation of Chongqing Municipal Education Commission under grant no. KJQN201900643 and no. KJQN201900630, the Chongqing Natural Science Foundation of Chongqing Municipal Science and Technology Bureau under grant no. cstc2020jcyj-msxmX0550, the Raised Fund Plan of National Natural Science Foundation of China of Chongqing University of Posts and Telecommunications grant no. A2020-528, the Research and training program for college students of Chongqing University of Posts and Telecommunications grant no. A2021-54.

References

[1] M. McCallum, A.C. Walls, K.R. Sprouse, J.E. Bowen, L. Rosen, H.V. Dang, A. deMarco, N. Franko, S.W. Tilles, J. Logue, M.C. Miranda, M. Ahlrichs, L. Carter, G. Snell, M.S. Pizzuto, H.Y. Chu, W.C. Van Voorhis, D. Corti, D. Veesler, Molecular basis of immune evasion by the Delta and kappa SARS-CoV-2 variants, Science 374 (2021) 1621–1626, https://doi.org/10.1126/science. abl8506.

[2] C. Motozono, M. Toyoda, J. Zahradnik, T. Ikeda, A. Saito, T.S. Tan, I. Ngare, H. Nasser, I. Kimura, K. Uriu, Y. Kosugi, S. Torii, A. Yonekawa, N. Shimono, Y. Nagasaki, R. Minami, T. Toya, N. Sekiya, T. Fukuhara, Y. Matsuura, G. Schreiber, S. Nakagawa, T. Ueno, K. Sato, An emerging SARS-CoV-2 mutant evading cellular immunity and increasing viral infectivity, bioRxiv (2021), https://doi.org/10.1101/2021.04.02.438288.

[3] A. Saito, H. Nasser, K. Uriu, Y. Kosugi, T. Irie, K. Shirakawa, K. Sadamasu, I. Kimura, J. Ito, J. Wu, S. Ozono, K. Tokunaga, E.P. Butlertanaka, Y.L. Tanaka, R. Shimizu, K. Shimizu, T. Fukuhara, R. Kawabata, T. Sakaguchi, I. Yoshida, H. Asakura, M. Nagashima, K. Yoshimura, Y. Kazuma, R. Nomura, Y. Horisawa, A. Takaori-Kondo, S. Nakagawa, T. Ikeda, K. Sato, SARS-CoV-2 spike P681R mutation enhances and accelerates viral fusion, bioRxiv 10 (2021) 17–448820, https://doi.org/10.1101/ 2021.06.17.448820.

[4] A.M. Tareq, T.B. Emran, K. Dhama, M. Dhawan, T.E. Tallei, Impact of SARS-CoV-2 Delta variant (B.1.617.2) in surging second wave of COVID-19 and efficacy of vaccines in tackling the ongoing pandemic, Hum. Vaccin. Immunother. 17 (2021) 1–2, https://doi.org/10.1080/21645515.2021.1963601.

[5] F. Li, R. Tao, B. Cao, L. Yang, L. Z. Wang, Manipulating the light-matter interaction of PtS/MoS2 p-n junctions for high performance broadband photodetection, Adv. Funct. Mater. 31 (2021) 2104367, https://doi.org/10.1002/adfm.202104367.

[6] X. Luo, Z. Peng, Z. Wang, M. Dong, Layer-by-layer growth of AA-stacking MoS2 for tunable broadband phototransistors, ACS Appl. Mater. Interfaces 13 (2021) 59154–59163, https://doi.org/10.1021/acsami.1c19906.

[7] L. He, J. Zhang, C. He, B. Zhao, W. Chen, S.R. Patil, Effect of cytosine hydroxymethylation on DNA charge transport, Mol. Cell Biochem. 476 (2021) 1599–1603, https://doi.org/10.1007/ s11010-020-03957-7.

[8] Y. Li, J.M. Artés, B. Demir, S. Gokce, H.M. Mohammad, M. Alangari, M. P. Anantram, E.E. Oren, J. Hihath, Detection and identification of genetic material via single-molecule conductance, Nat. Nanotechnol. 13 (2018) 1167–1173, https://doi.org/10.1038/s41565-018-0285-x.

[9] A.C. Walls, Y.J. Park, M.A. Tortorici, A. Wall, A.T. McGuire, D. Veesler, Structure, function, and antigenicity of the SARS-CoV-2 spike glycoprotein, Cell 181 (2020) 281–292, https://doi.org/10.1016/j.cell.2020.02.058.

[10] D. Wrapp, N. Wang, K.S. Corbett, J.A. Goldsmith, C.L. Hsieh, O. Abiona, B. S. Graham, J.S. McLellan, Cryo-EM structure of the 2019-nCoV spike in the prefusion conformation, Science 367 (2020) 1260–1263, https://doi.org/10.1101/2020.02.11.944462.

[11] S. Song, L. Ma, D. Zou, D. Tian, C. Li, J. Zhu, M. Chen, A. Wang, Y. Ma, M. Li, X. Teng, Y. Cui, G. Duan, M. Zhang, T. Jin, C. Shi, Z. Du, Y. Zhang, C. Liu, R. Li, J. Zeng, L. Hao, S. Jiang, H. Chen, D. Han, J. Xiao, Z. Zhang, W. Zhao, Y. Xue, Y. Bao, The global landscape of SARS-CoV-2 genomes, variants, and haplotypes in 2019nCoVR, Genom. Proteom. Bioinform. 18 (2020) 749–759, https://doi.org/10.1016/j.gpb.2020.09.001.

[12] Z. Gong, J.W. Zhu, C.P. Li, S. Jiang, L.N. Ma, B.X. Tang, D. Zou, M.L. Chen, Y. B. Sun, S.H. Song, Z. Zhang, J.F. Xiao, Y.B. Xue, Y.M. Bao, Z.L. Du, W.M. Zhao, An online coronavirus analysis platform from the National Genomics Data Center, Zool. Res. 41 (2020) 705–708, https://doi.org/10.24272/j.issn.2095-8137.2020.065.

[13] W.M. Zhao, S.H. Song, M.L. Chen, D. Zou, L.N. Ma, Y.K. Ma, R.J. Li, L.L. Hao, C. P. Li, D.M. Tian, B.X. Tang, Y.Q. Wang, J.W. Zhu, H.X. Chen, Z. Zhang, Y.B. Xue, Y. M. Bao, The 2019 novel coronavirus resource, Yi Chuan 42 (2020) 212–221, https://doi.org/10.16288/ j.yczz.20-030.

[14] D. Becker, A. Adhikary, M.D. Sevilla, The Role of Charge and Spin Migration in DNA Radiation Damage (1970), https://doi.org/10.1007/978-3-540-72494-0_7.

[15] J. Qi, M. Anantram, (Invited) Electron flow in GC8 DNA strand, ECS Trans. 64 (2014) 1–9, https://doi.org/10.1149/06412.0001ecst.

[16] Y. Xue, S. Datta, M.A. Ratner, First-principles based matrix-green's function approach to molecular electronic devices: general formalism, Chem. Phys. 281 (2002) 151–170, https://doi.org/10.1016/S0301-0104(02)00446-9.

[17] S. Baroni, P. Giannozzi, A. Testa, Green's-function approach to linear response in solids, Phys. Rev. Lett. 58 (1987) 1861–1864, https://doi.org/10.1103/PhysRevLett.58.1861.

[18] M.J. Frisch, G. Trucks, H.B. Schlegel, G.E. Scuseria, M.A. Robb, C. James, S. Giovanni, B. Vincenzo, M. Benedetta, G.A. Petersson, H. Nakatsuji, C. Marco, X. Li, H.P. Hratchian, A.F. Izmaylov, B. Julien, Z. Guishan, S. Jason, H. Masahiko, F. Douglas, Gaussian 09 Revision A.1. Gaussian Inc, 2009.

[19] R. Flores-Moreno, E. Posada, F. Moncada, J. Romero, J. Charry, M. Díaz-Tinoco, S. González, N. Aguirre, A. Reyes, LOWDIN: the any particle molecular orbital code, Int. J. Quantum Chem. 114 (2014) 50–56, https://doi.org/10.1002/qua.24500.

[20] L. He, J. Zhang, C. He, B. Zhao, Z. Xie, W. Chen, M.R. Sonawane, S.R. Patil, Electronic characteristics of BRCA1 mutations in DNA, Biopolymers (2021) https://doi.org/10.1002 /bip.23465.

[21] S.R. Patil, V. Chawda, J. Qi, M.P. Anantram, N. Sinha, Charge transport through DNA based electronic barriers, AIP Conf. Proc. (2018). https://doi.org/ doi: 10.1063/1.5033323.

[22] T. Lu, F. Chen, Multiwfn: a multifunctional wavefunction analyzer, J. Comput. Chem. 33 (2012) 580–592, https://doi.org/10.1002/jcc.22885.

[23] Y. Li, J.M. Artés, J. Qi, I.A. Morelan, P. Feldstein, M.P. Anantram, J. Hihath, Comparing charge transport in oligonucleotides: RNA:DNA hybrids and DNA duplexes, J. Phys. Chem. Lett. 7 (2016) 1888–1894, https://doi.org/10.1021/ acs.jpclett.6b00749.